VSP case study of a Leduc reef margin

Ronald C. Hinds*

and

Neil L. Anderson+

* Department of Geology, University of Pretoria, Pretoria, South Africa 0002
\+ Kansas Geological Survey, University of Kansas, Lawrence, Kansas 66047

Abstract

On the basis of the misinterpretation of conventional surface seismic data, an exploratory well (referred to as the VSP well) was drilled in the Ricinus area, southern Alberta, Canada. The prognosis prior to drilling, was that the VSP well would encounter the updip, raised rim of the Leduc Formation (Devonian Woodbend Group) reef complex at Ricinus Field, and would penetrate on the order of 140 m of gas pay. To the consternation of the explorationists, the well was drilled to the northeast of the Ricinus reef complex and encountered only offreef shales.

Prior to abandonment, two vertical seismic profiles (near-offset: 199 m; far-offset: 1100 m) were conducted at the VSP well site. These data were acquired in an effort to: 1) resolve the apparent discrepancy between the interpreted surface seismic data and the geology at the VSP well; and 2) evaluate the feasibility of whipstocking the VSP well in the direction of the reef complex. Towards these ends, the VSP was relatively successful. These data allowed for the more confident and geologically consistent reinterpretation of the surface seismic data, and clearly indicated that whipstocking was not an economically viable option.

Introduction

The Woodbend Group in central Alberta (Figure 1) is subdivided into four formations: Cooking Lake, Duvernay, Leduc, and Ireton. The Cooking Lake is platform facies, the Leduc is reefal facies, the Duvernay and Ireton are inter-reef shales (Anderson et al., 1989a and b: Klovan, 1964; McNamara and Wardlaw, 1991; Moore, 1988, 1989a, 1989b; Mossop, 1972; Mountjoy; 1980; Stoakes; 1980; Stoakes and Wendte, 1987).

The Leduc Formation at Ricinus (Figures 2 and 4), is classified as a large atoll. It towers some 350 to 400 m (based on 6-9-34-8 W5M) above the Cooking

Lake platform and appears to exhibit a mappable raised rim (peripheral rim) and a structurally lower central lagoonal area. (Such raised rims are described in Mossop (1972), in his study of the isolated Leduc Formation limestone reef complex at Redwater, as primarily the result of the differential compaction of rigid reef rim facies and central lagoonal facies.) The updip edge (northeast) of the raised rim at Ricinus is productive where it is structurally closed and effectively sealed by the inter-reef shales of the Duvernay and Ireton. The schematic cross-section of Figure 4 illustrate the interpreted morphological relationships between the Leduc and the inter-reef shales of the Ireton and Duvernay in the Ricinus area. The location of the schematic cross-section is shown in Figure 3.

In those areas of western Canada where the Devonian and/or overlying rock record is relatively undisturbed structurally, full Leduc reefs can usually be differentiated on seismic data from inter-reef shales. These carbonate buildups are typically characterized by appreciable velocity pullup (up to 25 ms), significant structural drape at the top of the Devonian (up to 70 ms), and character variations within the Woodbend Group (Anderson and Brown, 1987). Back from the steeply dipping edge, the top of these reefs is generally manifested on seismic data as a high-amplitude trough on reverse polarity data. In those areas where extensive structural deformation has occurred in the subsurface, the seismic image of the Leduc may be effectively masked by the superposed seismic signature of the structural complexities and can be difficult to define. Thrust faulting within Mesozoic strata in the general Ricinus area for example, can significantly affect the seismic signature of the Leduc reefs.

In this paper we present a case history that illustrates the potential for the misinterpretation of 2-D surface seismic data in the Ricinus area. This study is based on a situation where the plausible, yet ultimately inaccurate interpretation of surface seismic data led to the drilling of the VSP well. The VSP well was expected to intersect the updip edge of the Ricinus Leduc reef, unfortunately it encountered only offreef shales and was abandoned. Herein we discuss the VSP well results, and the surface seismic and VSP signatures at the VSP well site. The

2-D data presented were acquired prior to drilling the exploratory VSP well. The VSP survey was run in an attempt to resolve the discrepancy between the initial (pre-VSP well) interpretation of the surface seismic data and the geology at the VSP well site.

Ricinus Full Leduc reef

The geologic cross-section of Figure 4, summarizes the geophysical interpretation at the VSP well site prior to the drilling of the VSP well. This cross-section was based on the initial (pre-VSP well) interpretation of the example seismic data (Figure 5), and well control available at that time. The location and corresponding CDP numbers for the example seismic line (Figure 5 and 7) is shown in Figure 3. In this initial interpretation, full Leduc reef is present at the VSP well site. Ultimately, drilling confirmed that the VSP well site is offreef and that this initial seismic-based interpretation is incorrect.

On the initial interpreted version of the seismic data (Figure 5), the northern edge of the Leduc complex is located near trace 242, and full reef is mapped as present at the VSP well site. This erroneous interpretation appears to be supported by the patterns of time-structural relief observed along the more prominent seismic events. For examples, the near-Cambrian and Cooking Lake reflections appear to be pulled up by about 15 ms immediately to the south of trace 242, and the Ireton, Wabamun, Nordegg and Blairmore events appear to drape by up to 25 ms across the interpreted northern edge of the reef. Note that the anomalous structure at the Blairmore and Nordegg levels to the south of trace 314 in Figure 5, has been incorrectly attributed to thrust faulting within the Mesozoic section. This misinterpretation is consistent with the regional geology; Ricinus is situated immediately to the east of the line demarcating the eastern limit of Devonian thrust faulting, and structural deformation of varying intensity is observed within the Mesozoic strata in this area.

The geologic section of Figure 6 illustrates the morphology of the Ricinus

*complex as interpreted after the drilling of the offreef VSP well. This geologic section is constrained by well control and is based on the post-VSP interpretation of the example seismic line (Figure 7). Wells 6-9 and 7-15 (Figure 3) were drilled into full reef and are productive; 6-9 encountered approximately 22 m of gas pay within the Leduc, 7-15 encountered 140 m of pay (7-15 penetrated 250 m of Leduc reef). The VSP well (Figures 3 and 6) is off-reef, and encountered a full section of inter-reef shale (Ireton and Duvernay; Figure 1). The VSP well and 6-9 encountered Cooking Lake platform; however 7-15 was not drilled deep enough.

On the post-VSP well version of the seismic data (Figure 7), the northern edge of the Leduc complex is located near trace 314; the VSP well site is interpreted as offreef. This interpretation is supported by the patterns of time-structural relief observed along the more prominent seismic events. For examples, the Near-Cambrian and Cooking Lake reflections appear to be pulled up by up to 40 ms to the south of trace 314; the Ireton, Wabamun, Nordegg and Blairmore events appear to drape by up to 70 ms across the interpreted northern edge of the reef. Note that the time-structural relief observed at the Blairmore and Nordegg levels to the south of trace 314, is interpreted as drape and attributed to the differential compaction of reef and offreef sediment. In this interpretation, Mesozoic thrust faulting has not appreciably affected the rock record.

The interpreted 12-fold surface seismic data displayed in Figures 5 and 7 were acquired using a source pattern consisting of five 1-kg charges spread over 60 m. The shot interval was 120 m; the average shot depth was 9 m. The geophone groups consisted of nine inline 14-Hz geophones over 30 m; the group interval was 30 m. 96 traces were recorded using DFS-V recording equipment and a split-spread geometry; the near offset was 30 m. The field anti-aliasing filter for the surface seismic was OUT/128 Hz. The surface seismic datum in the area was 1400 m asl. The refraction statics replacement velocity used to reduce the surface seismic data to the seismic datum was 3350 m/s. The display presented as Figure 7, represents the post-VSP well interpretation of the seismic data and is markedly different than the interpretation prior to drilling.

VSP acquisition

After the analysis of the well log data and prior to abandonment, two VSP surveys were run at the VSP well site in order to:

(1) More accurately tie the surface seismic to the subsurface geology;

(2) Determine if the reef crest was within 500 m of the VSP well in the direction of the example seismic line (with a view to whipstocking); and

(3) Differentiate primary reflections from both surface-generated and interbed multiples.

The near-offset was 199 m from 13-15, the far-offset was 1100 m; both were online with respect to the surface seismic line (Figure 3) and in the direction of 5-22 to the southwest. Two Vibroseis units were operated in series at each offset. The 20 s sweep ranged from 8 to 80 hz, the recording length was 16 s, and the cross-correlated output was 4 s. Six to eight sweeps were summed for each geophone sonde location. The SSC 1078 VSP recording system were used. The sampling rate from the A/D digitizer was 2 ms. The recording filter was OUT/OUT.

The total depth of the VSP well was 4260 m below KB (KB was 1317 m ASL). The source elevation of both offsets was 1304 m ASL. The geophone sonde was lowered to the bottom of the well and normally raised at 30 m intervals. (Above 420 m, the depth spacing was 60 m up to the shallowest level of 180 m.) At each sonde location, the three component geophone tool was locked in place. Records were recorded at selected depths as the sonde was lowered down the borehole; these sonde locations were repeated during the production run. The use of these dual recording locations facilitates the detection of cable stretch or cable depth counter malfunction, and provides information regarding the gain

amplification that will be required during the VSP production run.

Near-offset (199 m) VSP interpretive processing

During the processing of the near-offset VSP a series of interpretive processing panels (IPPs) were generated to display the following:

(1) upgoing and downgoing P-wave separation;

(2) deconvolution of the separated upgoing P-waves using an inverse filter calculated from the separated downgoing P-waves; and

(3) inside and outside corridor stacks of both the deconvolved and nondeconvolved upgoing P-waves.

Throughout the paper, the abbreviations FRT, -TT time and +TT time (Hinds et al., 1989) are used repeatedly. FRT is the abbreviation for field recorded time, the term used to describe the time-depth display of the raw field records. The terms -TT and +TT refer to specific data configurations. -TT is used in reference to the display on which the first breaks and downgoing waves are horizontally aligned and bulk shifted. On these displays, the first break times have been subtracted from each trace, and the aligned traces have been bulk-shifted to an arbitrary time-datum (usually to 100 or 200 ms). +TT is used in reference to the display on which the first break time of each trace has been added to that trace (plus possible NMO corrections). On the +TT displays, the upgoing waves are aligned and should be in pseudo two-way traveltime. Unless otherwise noted, the VSP data displays are reverse polarity.

P-wave separation

The separation of upgoing and downgoing P-waves (vertical (Z) geophone data) is depicted in the wavefield separation interpretive processing panel or IPP

(Hinds et al., 1989) of Figure 8.

Panel 1 displays the raw Z data in field recorded time (FRT) after trace normalization. In panel 2, these data have been gained and several prominent primary upgoing events have been identified: Blairmore coals, Nordegg, Ireton and acoustic basement (crystalline Precambrian). With respect to the event identified as acoustic basement, note that this event originated below the base of the VSP well. As a result, it does not intersect the first break curve and cannot be positively identified as a primary reflection. The uncertainty as to the exact time depth to crystalline basement cannot be resolved without VSP control at that depth.

What is also bothersome about interpreting the acoustic basement reflector is the association of the downgoing surface generated multiple (that lags the first break by approximately 0.3 s) to the upgoing events recorded below TD. On panel 2, the downgoing multiple event that intersects the deepest trace at 1.05 s coincides with the upgoing wave that begins at 1.05 s and ends on the shallowest trace at 1.65 s. The implication is that some of the events recorded below the bottom may be multiple reflections from the bottom of the borehole itself.

In panel 3 (Figure 8), the combined wavefields are displayed such that the first breaks and downgoing P-wave multiple events are horizontally aligned. The gained raw VSP data presented in panel 3 illustrate that the downgoing wavetrain consists of the primary downgoing wavelet plus high-amplitude surface generated multiples and less prominent interbed multiples. The surface generated downgoing multiples are recognized as those horizontally aligned, post-first break arrivals that are recorded on all of the traces. If a downgoing multiple does not extend over the entire depth range but is evident on the deeper traces only, then that multiple is interpreted to be an interbed multiple (Hinds et al., 1989).

In the subsequent processing step, an 11-point median filter was used to remove the upgoing P-waves; the output separated and scaled downgoing waves are

displayed in panel 4. Note that the residual upgoing wave content in panel 4 is minimal. This panel is one of the most important panels for VSP interpretive processing. If residual upgoing wave remains in the separated downgoing wave panel, then that amount of residual upgoing wave is subtracted out of the upgoing wave data (panel 3) during wavefield separation. As mentioned above, the multiples that appear on all of the traces are most likely surface generated. This is the case for multiples down to 0.45 s. Beyond that time on panel 4, surface generated and interbed multiples (as seen between 0.75 and 0.9 s) exist.

In the next step of wavefield separation, the downgoing P-wave data of panel 4 were subtracted from the combined wavefield (panel 3) to yield the output upgoing wavefield (panel 5). The upgoing waves and downgoing shear waves (both primary and multiples) are shown in panel 5. The downgoing shear waves (SV) may have been generated at the bottom of the surface casing or near the surface. An example of a downgoing SV appears on the shallowest trace on panel 5 at 0.2 s (-TT time) and trends opposite to the upgoing events (deeper in time from left to right). Since the downgoing P-wave events have been horizontally aligned in a -TT display, the downgoing SV events are interpreted by their steeper slopes inferring a lower apparent velocity than the downgoing P-wave events.

The upgoing waves before and after the application of a 3-point median filter are shown in panels 6 and 7, respectively. The equalized amplitudes of the horizontally aligned upgoing waves for the Blairmore coals, Nordegg, Wabamun, Ireton, inter-Ireton, Cooking Lake, and acoustic basement events are interpreted in panel 7. One can note that the downgoing SV events seen in panel 5 dip more steeply in the +TT display; however, these events have been effectively attenuated by the application of the median filter. The Wabamun and Cooking Lake events have been identified only on traces deeper than the Nordegg due to multiple interference (to be discussed below).

VSP deconvolution

On VSP data, the initial downgoing pulse (except in the case of head wave contamination) is the primary downgoing P-wave; any later arriving, downgoing events are multiples (apart from downgoing shear or converted waves). Ideally, P-wave multiples can be effectively filtered using a deconvolution operator derived from an analysis of the separated downgoing P-wave wavetrain (Hardage, 1985; Hinds et al., 1989). Deconvolution also increases the dominant frequency of data, allowing for better vertical resolution.

The deconvolution IPP (Figure 9) enables the interpreter to monitor the deconvolution process. The incorporated panels reveal information (about multiples) that was difficult to determine from the wavefield separation IPP (Figure 8) alone. The first two panels (Figure 9) are the nonmedian and median filtered, nondeconvolved upgoing wavefields, respectively. Panel 3 is the gained combined wavefield (-TT aligned). Panels 4 and 5 are the nondeconvolved and deconvolved, upgoing wavefields, respectively. Both panels 4 and 5 are contaminated with downgoing shear waves. A comparison of these panels illustrates that the deconvolution process has enhanced the frequency content of the upgoing waves and preserved the primary reflections.

The last two panels (6 and 7) are the deconvolved, upgoing, nonmedian and median filtered data, respectively. A comparison of panels 2 and 7 (Figure 10), elucidates the effect of the Blairmore coal or Nordegg multiples on the continuity of primary reflections.

Multiple contamination is most noticeable at the Wabamun and Cooking Lake level. On panel 2, the Wabamun is relatively unaffected on traces that are recorded below the Nordegg depth of 3466 m (-2151 masl). The upgoing multiple reflection from the Nordegg will not be detected on traces deeper than the bottom generating layer of the interbed (the Nordegg) because, by our definition, the multiple is an upgoing wave, not downgoing.

Just below the inter-Ireton trough in panel 2 on the traces from depth 3466

m to the bottom of the borehole is a trough interpreted to be the Cooking Lake event. The Cooking Lake interpretation is supported by the sonic log/synthetic seismogram Cooking Lake correlation to the surface seismic shown in Figure 7. What effect does deconvolution have on these events; Wabamun and Cooking Lake?

On panel 7, we see that the Wabamun event is laterally continuous and can be correlated on all depth traces as a result of the deconvolution. The Cooking Lake event (trough) can now be confidently interpreted.

In the zone of interest around the Ireton event, the multiple contamination is minimal. The inter-Ireton is continuous and does not exhibit significant structure either before or after the VSP deconvolution.

Inside and outside corridor stacks

Multiple contamination can also be analyzed on inside and outside corridor stacks. Inside corridor stacks of nondeconvolved data contain both primaries and multiples. Nondeconvolved outside corridor stacks are predominated by primary events (except in the case of severe head-wave contamination). Ideally, deconvolved inside and outside corridor stacks will contain primary events only.

Nondeconvolved, inside and outside corridor stacks and associated displays are presented in Figure 10. A comparison of the outside and inside corridor stacks (panels 3 and 4, respectively) illustrates the utility of these displays. For example, the multiple interference generated by the Blairmore or Nordegg interbed multiple can interpreted on the inside corridor stack but is not seen on the outside corridor stack. On the outside corridor stack, the Wabamun trough dominates (at 1.85 s); however the inside corridor stack at the same time shows no semblance of a Wabamun event.

On the unmuted input data for the corridor stack displays (Figure 10, panels

1 and 6) we can note that the Cooking Lake event exists as a trough beneath the inter-Ireton event (trough). The event is so weak without the deconvolution that even the outside corridor stack does not show the Cooking Lake trough. This is the reason for also displaying the unmuted input data in the corridor stack IPP.

On the deconvolved data corridor stack panels (Figure 11), the Wabamun and Cooking Lake events can be interpreted.

If deconvolution is successful, the deconvolved, outside and inside corridor stacks (panels 3 and 4; Figure 11) should be similar. The inside and outside deconvolved corridor stacks show that the surface generated multiples have been substantially attenuated by the VSP deconvolution process; however there is enough difference between the two stacks to predict that the interbed multiples have been simply attenuated but not totally removed.

The deconvolved data and the corridor stacks show that the Wabamun and Cooking Lake primaries are flat lying continuous upgoing primary events across the entire VSP panel once the effect of the multiple is minimized. At this point the surface seismic can be reinterpreted at the well location.

Far-offset (1100 m) VSP interpretive processing

On the far-offset VSP data, the vertical (Z), and both horizontal (X and Y) axis contain nonpartitioned elements of the upgoing and downgoing P- and SV-wavefields. Examination of the IPPs (Figures 12-14) reveals that the partitioning of the wavefields (both up- and downgoing P and SV events) has significant implications with respect to interpretation.

As seen in panel panels 5 and 6 of the near-offset wavefield separation IPP shown in Figure 8, a downgoing SV wave (trending in the opposite direction to the upgoing waves in panel 5) is noticeable. Normally, downgoing and upgoing shear waves are not seen on near-offset data. We can therefore expect shear wave

contamination to be readily noticeable on the far-offset data. The partitioning of the wavefields presented below will play an important role in isolating the P upgoing waves from both the P and SV downgoing waves and upgoing shear waves.

Below the far-offset IPPs are discussed and the following routine interpretive processing steps displayed:

1) hodogram-based rotation of the X, Y, and Z data (based on windowed data enveloping the P-wave first arrival; DiSiena et al., 1984);

2) time-variant model-based rotations applied to the $HMAX_{up(derot)}$ and $Z_{up(derot)}$ data; and

3) the VSP-CDP transformation of the data (Dillon and Thomson, 1984).

Hodogram-based rotation

The raw X, Y, and Z data for the far-offset VSP are displayed in Figure 12 as panels 1, 2, and 3, respectively. The X and Y datasets contain both P and SV downgoing waves plus recognizable upgoing SV events. These upgoing SV events can be seen on both panel 1 and 2 originating at depth levels 2790 and 3300-3300 m. These events slope differently to the upgoing P wave events seen on panel 3. The partitioned downgoing primary P waves (first breaks wavelet) are consistent on both the X and Y datasets in panels 1 and 2 on traces recorded in the upper two-thirds of the borehole. The first breaks of the X and Y data indicate that the tool was rotating on the deeper depth traces. This is indicated by the first breaks becoming inconsistent on a single panel. In panel 3, the Z axis first breaks are phase consistent.

The first step, illustrated in Figure 12, is the hodogram-based rotation of the X and Y data (this corrects for first break inconsistencies due to the rotation of the

tool during the movement of the sonde up the borehole by projecting data from both of the input channels onto an axis which lies in the plane defined by the borehole and the source; namely the HMAX data panel). The output HMIN and HMAX data are displayed as panels 4 and 5, respectively. HMIN and HMAX data are assumed to be aligned perpendicular and tangent to the plane formed by the source and wellbore, respectively. Note that HMIN (comprised of horizontally polarized shear (SH) wave events and out of the plane reflections), contains possible downgoing SV waves (appearing on the shallow traces at 0,6 s) that could originate at the casing joints or upgoing waves that originate out of the plane of the well.

The remnant of a mode-converted downgoing SV wave with components along the HMIN axis appears at the Nordegg and Blairmore level. The upgoing SV events from the Nordegg and Blairmore coals that were first noticed on both of the X and Y panels are now more noticeable after redistribution onto the HMAX axis. Unfortunately, the downgoing SV events on the HMAX panel are of equal amplitude to the downgoing P waves. The HMAX panel contains consistent polarized downgoing P wave first breaks as the data of the input X and Y channel data have been rotated into the plane containing the downgoing P wave.

The Z' (panel 6) and HMAX' (panel 7) data were obtained by rotating the Z and HMAX data using polarization angles estimated from a hodogram analysis of data within a window around the P-wave first arrival (DiSiena et al., 1984). This technique is designed to polarize the data so that the downgoing P- waves are effectively isolated on a single channel, HMAX' (panel 7).

On the HMAX' data in panel 7 of Figure 13, the downgoing P wave energy is dominant. The HMAX' panel contains residual downgoing shear (SV) waves (converted to SV waves at the Blairmore coal interface) and upgoing P wave energy. This indicates that the polarization required to delineate the downgoing P wave data onto a single panel is not adequate to separate the upgoing P wave data entirely onto the orthogonally aligned Z' panel.

The Z' data shown in panel 6 contains downgoing shear wave and upgoing P wave energy that fit the assumption that the primary upgoing P waves are orthogonal to the primary downgoing P waves (isolated on the HMAX' panel). The downgoing shear wave overshadows the lower amplitude upgoing P wave. The time-variant polarization of the data (modelled on the upgoing P waves) will attempt to detach the contaminating up- and downgoing shear waves from the upgoing P waves and isolate the upgoing P waves onto a single output data panel, Z''_{up}.

Time-variant model-based rotation

The time-variant model-based polarization analysis interpretive processing panel is shown in Figure 14. The separated (using an FK filter), upgoing events from the Z' and HMAX' data are shown in panels 1 and 2, respectively. These data are referred to as Z'_{up} and $HMAX'_{up}$. These panels are compared to the final two panels (5 and 6) containing the time-variant model-based polarized $HMAX''_{up}$ and Z''_{up} data. The emphasis is on the improvement of the quality of the upgoing P waves on the Z''_{up} panel.

In order to remove the effects of the Z to Z', and HMAX to HMAX' transformations (used in isolating the downgoing P-waves), the Z'_{up} and $HMAX'_{up}$ were derotated (using the inverse operation of the second polarization rotation). The output data of the derotation process, namely $HMAX_{up(derot)}$ and $Z_{up(derot)}$, are shown as panels 3 and 4 of Figure 13, respectively. The upgoing P-wave events have been effectively distributed back onto a Z-type axis, $Z_{up(derot)}$. Unlike the upgoing wave events in the raw Z data (panel 3 in Figure 12), where the downgoing P-waves were predominant, the separated upgoing P-wave events in the $Z_{up(derot)}$ data are dominant and interpretable.

On the $Z_{up(derot)}$ data (panel 4), upgoing P-waves generated by shallow reflectors are improperly aligned (due to the choice of non-time variant rotation angles). These data have been derotated but the upgoing P-wave events are still partitioned on both output data ($Z_{up(derot)}$ and $HMAX_{up(derot)}$) due to the non-zero offset of the source. The deeper events do not suffer much misalignment because deep event raypath geometries satisfy the near-vertical incidence angle assumption better than the raypaths of shallower events. The time-variant model-based rotation corrects for this misalignment of the shallow events. The output upgoing wave displays, $HMAX''_{up}$ and Z''_{up}, are shown on panels 5 and 6, respectively. Note that the shallow events display better alignment than on the $Z_{up(derot)}$ (panel 4). The rotation angle required for the Blairmore coals event on a particular trace was different to the rotation angle for deeper events (such as the acoustic basement) on the same trace. The time-variant rotation technique generated these different rotation angles.

The most realistic approximation to a far-offset VSP deconvolution uses the separated polarized downgoing waves ($HMAX'_{down}$) and the separated time-variant polarized upgoing P waves (Z''_{up}). The deconvolution process proceeds by designing the inverse wavelet for the downgoing waves of the HMAX' panel (Figure 12) and applying the operator to the Z''_{up} data (Figure 13).

The deconvolution was performed on the Z''_{up} far offset data; however the process added unacceptable noise to the data. The interpretation is done on the non-deconvolved far-offset VSP data as it was interpreted that the multiple contamination was minimal at the zones of interest on the Z''_{up} data. For the far-offset VSP data, the Blairmore or Nordegg multiples

have a longer travel path to reach the Wabamun in comparison to the near-offset VSP data. The Wabamun seems to be less affected on the LSP data by the Blairmore coal or Nordegg multiple than on the near-offset VSP data for this reason. This results in the deconvolution process for the far-offset VSP data becoming a non-critical step.

VSP-CDP transformation

The Z''_{up} data is used for the interpretation of the off-reef markers. Two interpretation panels are used for this purpose. The first concentrates on the transformation of the Z''_{up} data in time (+TT) and depth into the VSP-CDP (Dillon and Thomson, 1984) domain of time (+TT) and offset distance from the well. The interpretive processing of the VSP-CDP transform is displayed in the VSP-CDP IPP of Figure 14. (The second interpretation panel is the integrated seismic display which merges the VSP-CDP display and the seismic)

The Z''_{up} data in panel 6 of Figure 13 placed in +TT time is shown as the first panel of the VSP-CDP IPP in Figure 14. Upgoing mode-converted SV event contamination is interpreted to be quite severe on this panel. Although the upgoing P wave events are horizontally aligned, the mode-converted SV events originating at the Nordegg level dissect the upgoing P wave events (below the Nordegg level) and degrade the interpretation of the data. An FK based filter was applied to the data (in panel 1 of Figure 14) to attenuate the upgoing (and downgoing) SV events; the output being displayed in panel 2. A median filtered version of the Z''_{up} data of panel 2 is displayed in panel 3. The VSP-CDP transformed (pseudo two-way traveltime vs. offset) data are shown as panel 4.

The Blairmore coal, Nordegg, Wabamun, Ireton, inter-Ireton, Cooking Lake and near-basement markers are interpreted on these presentations. The FK (panel 2) and median filtering (panel 3) plus the VSP-CDP transform processing (panel 4) have not appreciably distorted the interpretability of the original data ($Z"_{up}$ data in panel 1).

Usually, for far-offset VSP data, up- and downgoing primary or mode-converted SV energy is of equal or greater amplitude than the upgoing P energy. As a result of the SV event separation from the $Z"_{up}$ data, the P wave events will suffer destructive interference (dim spots) where the SV data had previously crossed the original data (both in the up- and downgoing directions). The resultant VSP-CDP of the $Z"_{up}$ filtered data must be interpreted with this SV wave attenuation processes in mind.

The Ireton and inter-Ireton events are interpreted to be continuous and relatively horizontal indicating that only off-reef events have been imaged from the far-offset VSP processed data.

Integrated interpretation

The integrated seismic display contains the surface seismic line merged with the VSP-CDP transformed results (panel 4 of Figure 12). The integrated seismic display (Figure 15) shows that the seismic interpretation shown in Figure 5 extended the interpretation of the edge of the reef too far to the northeast, and supports the current interpretation as Figure 7.

These data also illustrate that the off-reef inter-Ireton event evident on the seismic section (Figure 8) extends about 500 m to the Southwest. In comparison to the seismic, the quality of the far-offset VSP data is

degraded. This is due to the mode-converted SV wave contamination. The surface seismic processing would do a better job of attenuating the SV events through the processing steps of normal moveout correction and CDP stacking. In spite of the quality of the VSP data, the tie to the surface seismic up to 500 m away from the VSP well allows for the confident correlation of the inter-Ireton marker. Since a smaller bundle of rays has been affected by the Mesozoic faulting and the normal CDP coverage found in surface seismic is not done in VSP processing, the coverage of the far-offset VSP can be interpreted with a high level of confidence. By the processing that was applied in the rotations and the filtering using interpretive processing, the signal was enhanced enough to allow for an interpretation alongside the seismic data.

The offsets for the survey were selected with the following considerations in mind:

1) If the atoll edge was in the near vicinity, then the inter-Ireton marker would terminate against the reef flank;

2) If the reef was further than 500 m away from the borehole or if the reef was to the southwest of the borehole, the inter-Ireton marker would be relatively flat and continuous;

3) the multiple that would affect a zero-offset seismic interpretation (migrated section) would be evident on the zero-offset VSP results; and

4) the exact geological tie with the seismic would be interpreted using the zero-offset VSP data.

The 199 m offset enabled an interpretation of the seismic signature at the well with a minimum of seismic interference from the complex Mesozoic faulting. The energy travelling down to the sonde in the borehole, pass through the geological strata at near-normal incidence angles resulting in less ray bending than the CDP gathered surface seismic data. The well was in an off-reef position with the seismic interpretation being focused on the Ireton, inter-Ireton, and Cooking Lake rather than the Leduc. The overlying marker that is used in isochron interpretation was the Wabamun. The interpretational concern was that the Wabamun event was effected by the Blairmore coals or Nordegg multiples.

On the non-deconvolved VSP data, interference with the Wabamun occurred until the geophone was below the Nordegg. The upgoing VSP events tied with seismic section only after the VSP deconvolution was applied. This would indicate that the deconvolution operator for surface seismic changes according to offset geometry as the far-offset VSP upgoing events did not critically require deconvolution (using the separated HMAX' downgoing waves to design the operator).

The far offset VSP provided subsurface coverage for 500 m away from the VSP well site. Each trace represents approximately 6 m of subsurface coverage. The updated geological model based on the far-offset VSP results is shown in Figure 8. In this figure, 6-9 and 7-15 are reefal; the VSP well however, is at least 500 m away from the reef edge.

Figure 15 shows that the seismic marker for the inter-Ireton is continuous and displays relatively little structure. The event does not terminate against the flank of the reef on the merged far-offset VSP and

seismic section. The Wabamun event in the far-offset VSP data has not been affected appreciably by the multiples from the Blairmore coal zones due to the different geometry of the raypaths between the zero offset VSP and the far-offset VSP. The Leduc reef event dips relatively steeply to the north of 7-15 to the reefal platform position (Figures 7 and 15) suggesting an abrupt edge may be present beyond 500 m southwest of the VSP well.

The geological tie has been confidently interpreted from the IPP at the well location and the interpretation has been carried through to the merged far-offset VSP and seismic dataset in the ISD, all using the philosophy of interpretive processing. The mapping of the off-reef sediments has enabled the final whipstock decision to be made. The decision was to abandon the well because the reef was more than 500 m away from the well location.

Summary

On the basis of the misinterpretation of conventional surface seismic data, the VSP exploratory well was drilled. The prognosis prior to drilling, was that the VSP well would encounter the updip, raised rim of the Leduc Formation complex at Ricinus Field, and on the order of 140 m of gas pay. To the consternation of the geophysicists, the well was drilled to the north of the reef complex and encountered only offreef shales.

Prior to abandonment, two VSP (near-offset: 199 m; far-offset: 1100 m) surveys were conducted at the VSP well site. These data were acquired in an effort to:

1) resolve the apparent discrepancy between the interpreted surface

seismic data and geology at the VSP well; and

2) evaluate the feasibility of whipstocking the VSP well in the direction of the reef complex.

Towards these ends, the VSP was relatively successful. These data allowed for the more confident and geologically consistent reinterpretation of the surface seismic data, and clearly indicated that whipstocking was not an economically viable option. The profile data supplemented the surface seismic and well log control in that:

1) VSP data could be directly correlated to the surface seismic. As a result, the surface seismic control could be accurately tied to the subsurface geology; and

2) multiples could be identified on the VSP data and subsequently further analyzed on the surface seismic data.

The information provided by the VSP surveys allowed the geophysicists to refine their interpretation of the surface seismic data, and enabled the construction of a geologically consistent cross-section. These interpretations provide information with respect to the subsurface in the proximity of the VSP well.

References

AGAT Laboratories, 1988, Table of formations of Alberta: AGAT Laboratories, Calgary.

Anderson, N.L., and Brown, R.J., 1987, The seismic signatures of some western Canadian Devonian reefs: Journ. Can. Soc. Expl. Geophys. 23, 7-26.

Anderson, N.L., Brown, R.J., and Hinds, R.C., 1989a, Low- and high-relief Leduc Formation reefs: A seismic analysis: Geophysics 54, 1410-1419.

Anderson, N.L., White, D., and Hinds, R.C., 1989b, Woodbend Group reservoirs, *in* Anderson, N.L., Hills, L.V. and Cederwall, D.A., Eds, Geophysical atlas of western Canadian hydrocarbon pools: Can. Soc. Expl. Geophys./Can. Soc. Petr. Geol., 101-132.

Balch, A.H., and Lee, M.W., 1984, Vertical seismic profiling-techniques, applications and case histories: Int. Human Res. Devel. Corp., Boston, 488 p.

Beydoun, W.B., 1985, Asymptotic wave methods in heterogeneous media: unpubl. Ph.D. thesis, Mass. Inst. Tech..

Dillon, P.B., and Thomson, R.C., 1984, Offset source VSP surveys and their image reconstruction: Geophys. Prosp. 32, 790-811.

Hardage, B.A., 1985, Vertical seismic profiling: Geophys. Press, London, 2nd edition, 509 p.

Hinds, R.C., Kuzmiski, R.K., Botha, W.J., and Anderson, N.L., 1989, Vertical and lateral seismic profiles, *in* Anderson, N.L., Hills, L.V. and Cederwall, D.A., Eds, Geophysical atlas of western Canadian hydrocarbon
Hinds, R.C., 1991, Seismic signatures and integrated exploration: Newsletter of the South African Geophys. Assoc., July issue, 10-12.
pools: Can. Soc. Expl. Geophys./Can. Soc. Petr. Geol., 319-344.

Klovan, J.E., 1964, Facies analysis of the Redwater reef complex, Alberta, Canada: Bull. Can. Petr. Geol., 12, 2260-2281.

Moore, P.F., 1988, Devonian geohistory of the western interior of Canada, *in* McMillan, N.J., Embry, A.F. and Glass, D.J., Eds., Devonian of the World: Can. Soc. Petr. Geol. Memoir 14, 67-87.

Moore, P.F., 1989a, Devonian reefs in Canada and some adjacent areas, *in* Geldsetzer, H.H.J., James, N.P. and Tebbutt, G.E., Eds., Reefs, Canada and Adjacent areas: Can. Soc. Petr. Geol. Memoir 13, 367-390.

Moore, P.F., 1989b, The Kaskaskia Sequence: reefs, platforms and foredeeps, The lower Kaskaskia Sequence - Devonian, *in* Ricketts, B.D., Eds., Western Canada sedimentary basin, a case history: Can. Petr. Geol., 139-164.

Mossop, G.D., 1972, Origin of the peripheral rim, Redwater reef, Alberta: Bull. Can. Petr. Geol., 20, 238-280.

Mountjoy, E., 1980, Some questions about the development of Upper Devonian carbonate buildups (reefs), Western Canada: Bull. Can. Petr. Geol., 28, 315-344.

Stoakes, F.A., 1980, Nature and control of shale basin fill and its effect on reef growth and termination: Upper Devonian Duvernay and Ireton Formations of Alberta, Canada: Bull. Can. Petr. Geol., 28, 345-410.

Stoakes, F.A., and Wendte, J.C., 1987, The Woodbend Group, *in* Krause, F.F. and Burrows, O.G., Eds., Devonian lithofacies and reservoir styles in Alberta: Second International Symposium Devonian System, Calgary, 153-170.

LIST OF FIGURES

6: median filtered upgoing waves (+TT))

Figure 11. Interpretive processing panel illustrating the utility of the deconvolved inside and outside corridor stacks. (1: median filtered, deconvolved upgoing waves (+TT); 2: muted outside corridor deconvolved data (+TT); 3: outside corridor deconvolved stack; 4: inside corridor deconvolved stack; 5: muted inside corridor deconvolved data (+TT); 6: median filtered, deconvolved upgoing waves (+TT))

Figure 12. Interpretive processing panel depicting the hodogram-based rotation of the far-offset VSP. (1: X-axis (FRT); 2: Y-axis (FRT); 3: Z-axis (FRT); 4: HMIN (FRT); 5: HMAX (FRT); 6: Z' (FRT); 7: HMAX' (FRT)).

Figure 13. Interpretive processing panel depicting the time-variant model-based rotation of the far-offset VSP. (1: Z'_{up} (FRT); 2: $HMAX'_{up}$ (FRT); 3: $HMAX_{up(derot)}$ (FRT); 4: $Z_{up(derot)}$ (FRT); 5: $HMAX''_{up}$ (FRT); 6: Z''_{up} (-TT)).

Figure 14. Interpretive processing panel showing VSP-CDP transformation of the non-deconvolved far-offset VSP data. (1: Z''_{up} data (+TT); 2: Z''_{up} data (+TT) after FK filtering; 3: median filtered (of panel 2) Z''_{up} data (+TT); 4: Z''_{up} VSP-CDP (of panel 3) data (+TT)).

Figure 15. Integrated seismic display showing the VSP-CDP transformed far-offset Z''_{up} data merged with the surface seismic data. These VSP data replace CDP's 258-293.

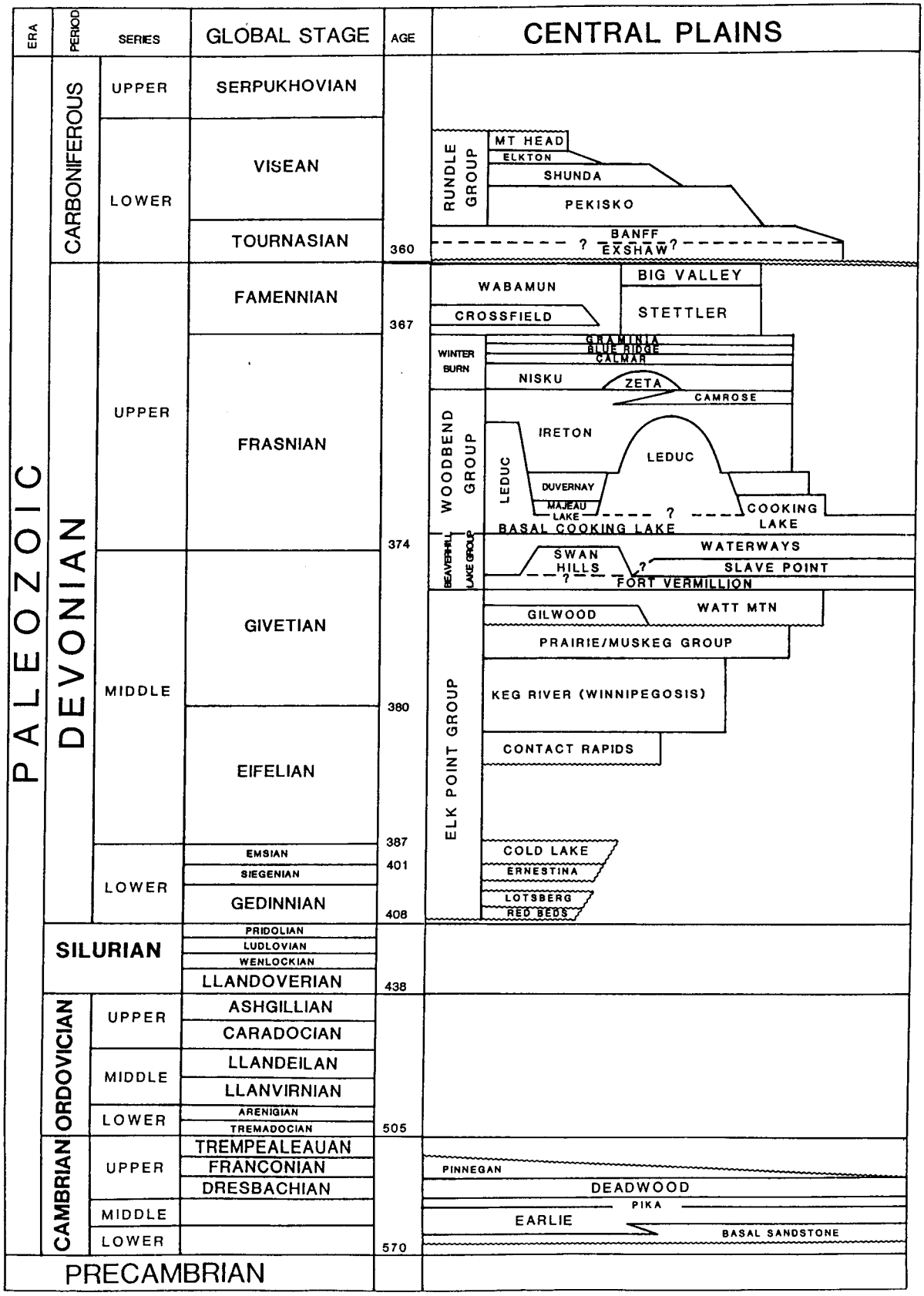
ERA
PERIOD
SERIES
GLOBAL STAGE
AGE
CENTRAL PLAINS
PALEOZOIC
CARBONIFEROUS
DEVONIAN
UPPER
LOWER
MIDDLE
SERPUKHOVIAN
VISEAN
TOURNASIAN
FAMENNIAN
FRASNIAN
GIVETIAN
EIFELIAN
EMSIAN
SIEGENIAN
GEDINNIAN
SILURIAN
PRIDOLIAN
LUDLOVIAN
WENLOCKIAN
LLANDOVERIAN
ORDOVICIAN
ASHGILLIAN
CARADOCIAN
LLANDEILAN
LLANVIRNIAN
ARENIGIAN
TREMADOCIAN
CAMBRIAN
TREMPEALEAUAN
FRANCONIAN
DRESBACHIAN
PRECAMBRIAN
360
367
374
380
387
401
408
438
505
570
RUNDLE GROUP
MT HEAD
ELKTON
SHUNDA
PEKISKO
BANFF
EXSHAW
WABAMUN
BIG VALLEY
CROSSFIELD
STETTLER
GRAMINIA
BLUE RIDGE
CALMAR
WINTER BURN
NISKU
ZETA
CAMROSE
WOODBEND GROUP
IRETON
LEDUC
DUVERNAY
MAJEAU LAKE
COOKING LAKE
BASAL COOKING LAKE
BEAVERHILL LAKE GROUP
SWAN HILLS
WATERWAYS
SLAVE POINT
FORT VERMILLION
ELK POINT GROUP
GILWOOD
WATT MTN
PRAIRIE/MUSKEG GROUP
KEG RIVER (WINNIPEGOSIS)
CONTACT RAPIDS
COLD LAKE
ERNESTINA
LOTSBERG
RED BEDS
PINNEGAN
DEADWOOD
PIKA
EARLIE
BASAL SANDSTONE

Figure 1

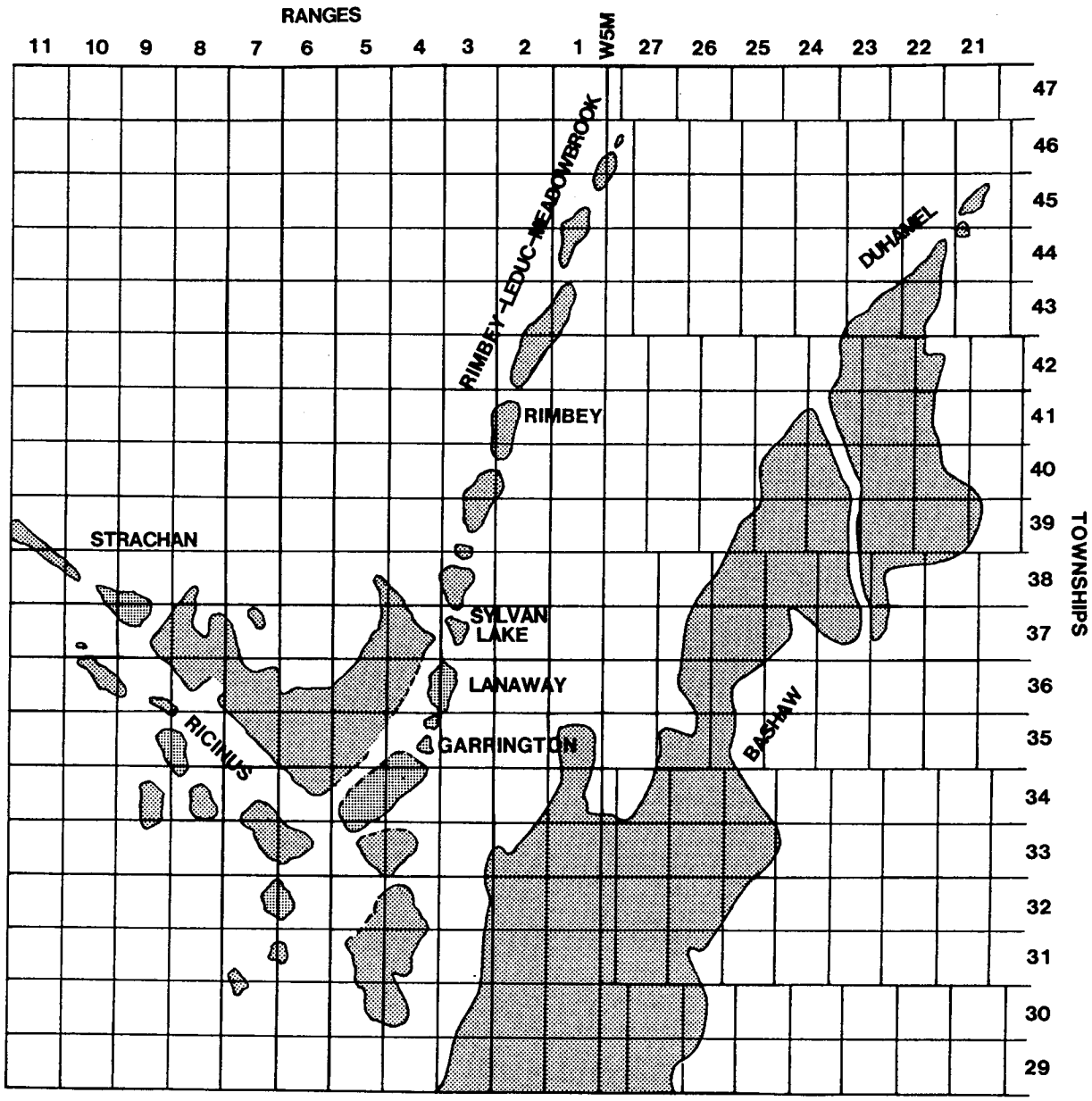
RANGES
11 10 9 8 7 6 5 4 3 2 1 W5M 27 26 25 24 23 22 21
47 46 45 44 43 42 41 40 39 38 37 36 35 34 33 32 31 30 29
TOWNSHIPS
RIMBEY-LEDUC-MEADOWBROOK
DUHAMEL
RIMBEY
STRACHAN
SYLVAN LAKE
LANAWAY
GARRINGTON
RICINUS
BASHAW

Figure 2.

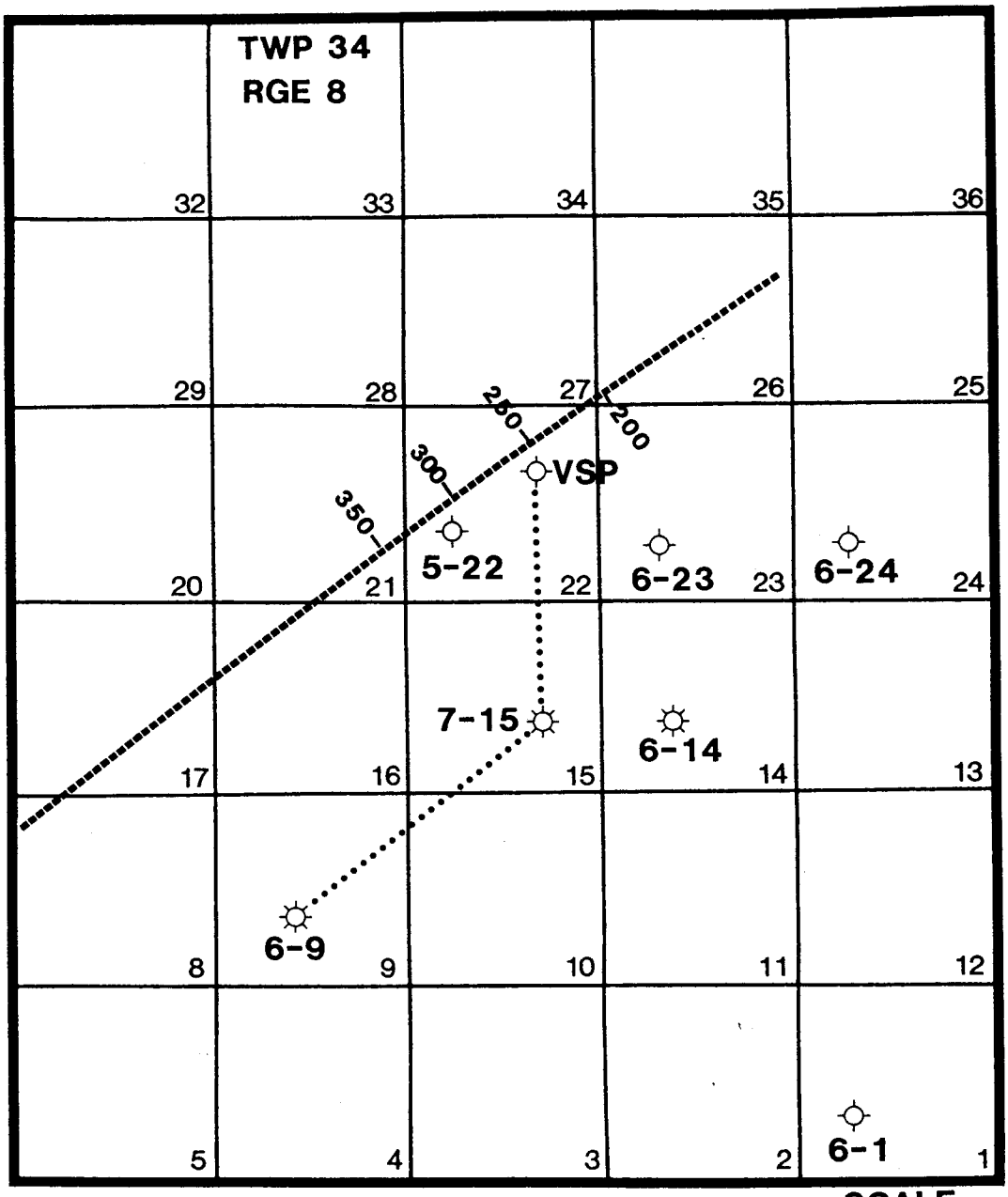
TWP 34
RGE 8
32
33
34
35
36
29
28
27
26
25
20
21
22
23
24
17
16
15
14
13
8
9
10
11
12
5
4
3
2
1
250
200
300
350
VSP
5-22
6-23
6-24
7-15
6-14
6-9
6-1
GEOLOGIC CROSS-SECTION
SEISMIC SECTION
SCALE
1 MILE

Figure 3.

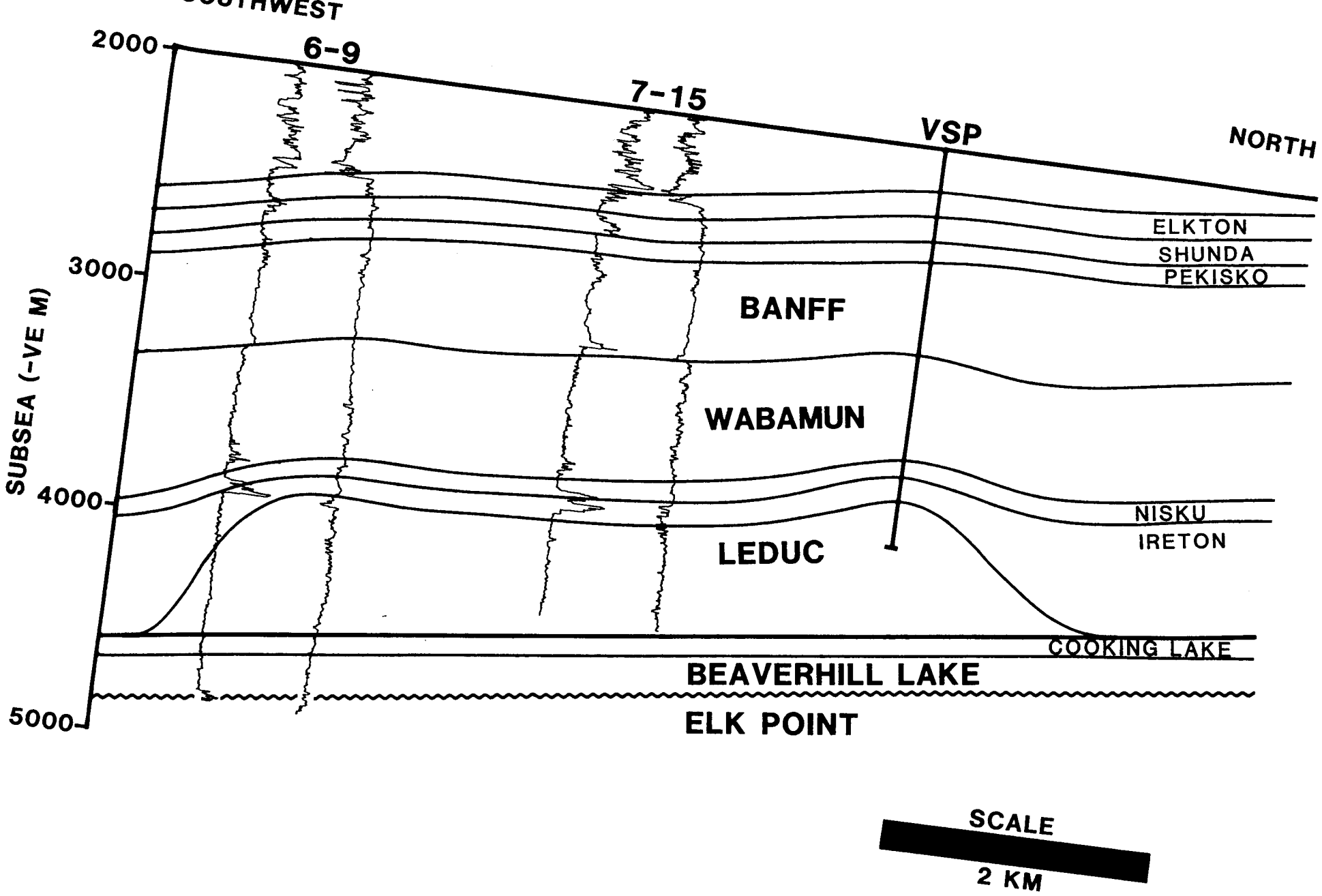
SOUTHWEST
2000
6-9
7-15
VSP
NORTH
ELKTON
SHUNDA
PEKISKO
3000
BANFF
SUBSEA (-VE M)
WABAMUN
4000
NISKU
IRETON
LEDUC
COOKING LAKE
BEAVERHILL LAKE
5000
ELK POINT
SCALE
2 KM

Figure 4.

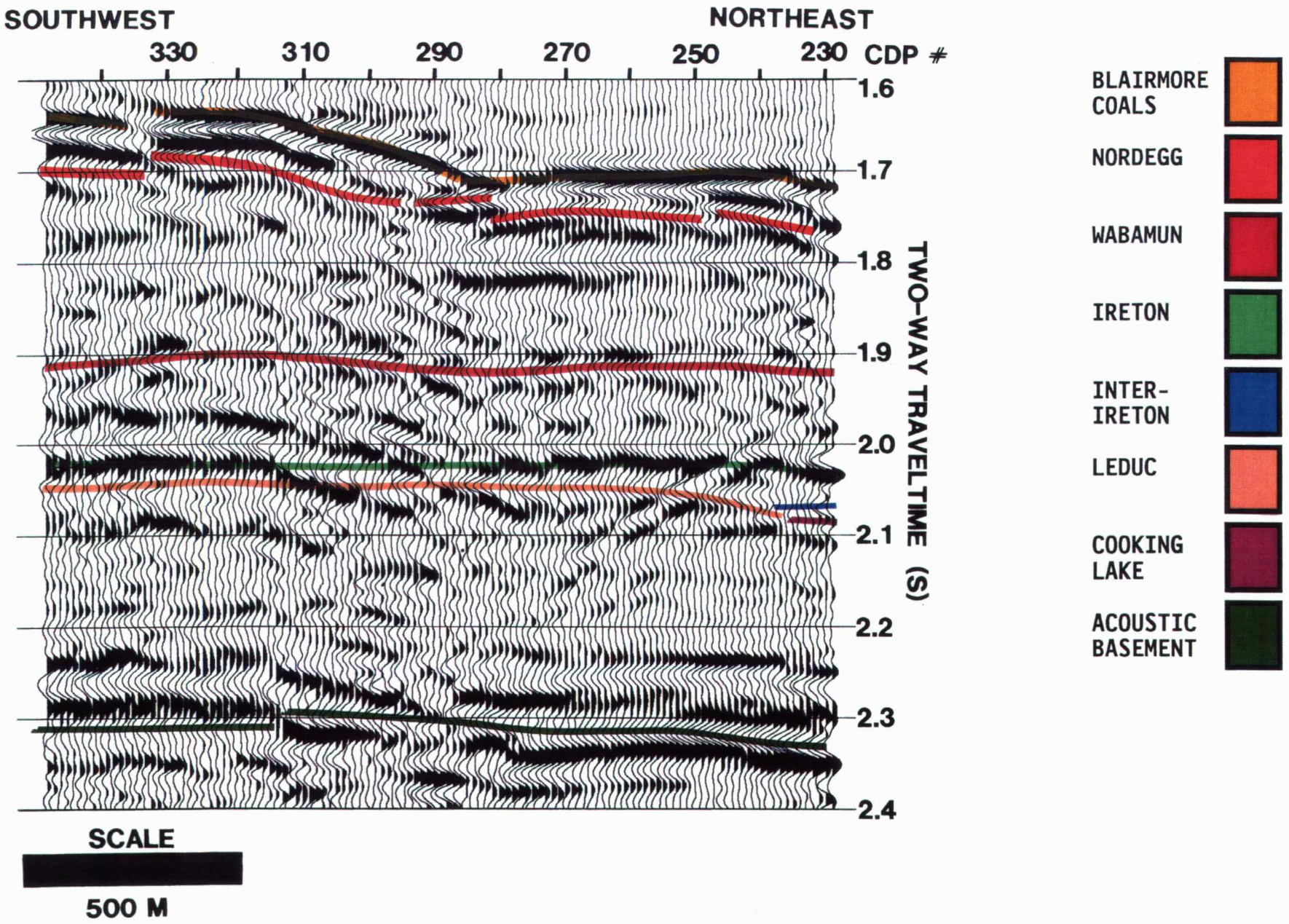
SOUTHWEST
NORTHEAST
330
310
290
270
250
230
CDP #
1.6
1.7
1.8
1.9
2.0
2.1
2.2
2.3
2.4
TWO-WAY TRAVELTIME (S)
SCALE
500 M
BLAIRMORE COALS
NORDEGG
WABAMUN
IRETON
INTER-IRETON
LEDUC
COOKING LAKE
ACOUSTIC BASEMENT

Figure 5.

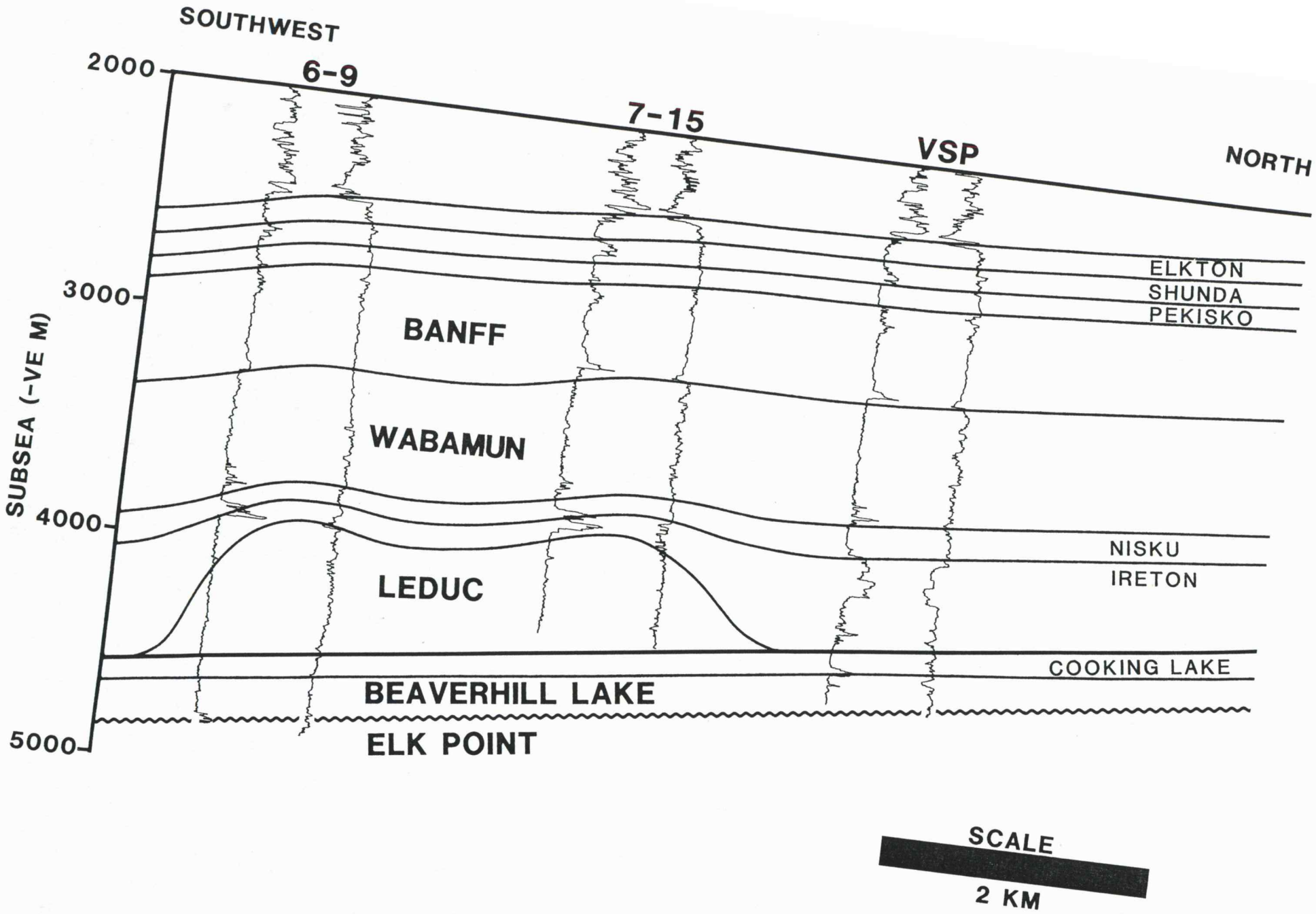
SOUTHWEST
2000
6-9
7-15
VSP
NORTH
3000
SUBSEA (-VE M)
BANFF
ELKTON
SHUNDA
PEKISKO
WABAMUN
4000
NISKU
IRETON
LEDUC
COOKING LAKE
BEAVERHILL LAKE
5000
ELK POINT
SCALE
2 KM

Figure 6.

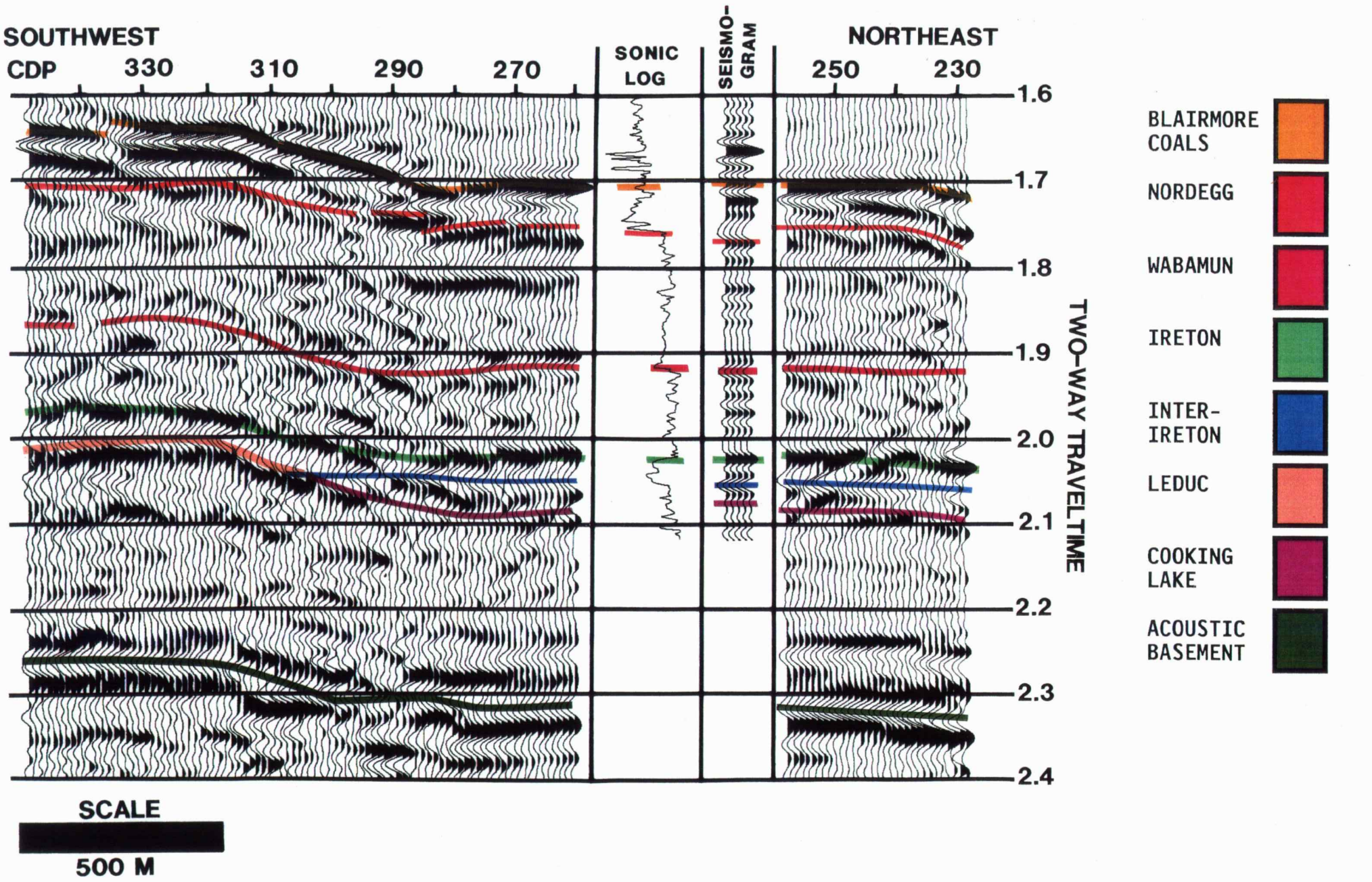
SOUTHWEST
CDP
330
310
290
270
SONIC LOG
SEISMO-GRAM
NORTHEAST
250
230
1.6
1.7
1.8
1.9
2.0
2.1
2.2
2.3
2.4
TWO-WAY TRAVELTIME
BLAIRMORE COALS
NORDEGG
WABAMUN
IRETON
INTER-IRETON
LEDUC
COOKING LAKE
ACOUSTIC BASEMENT
SCALE
500 M

Figure 7.

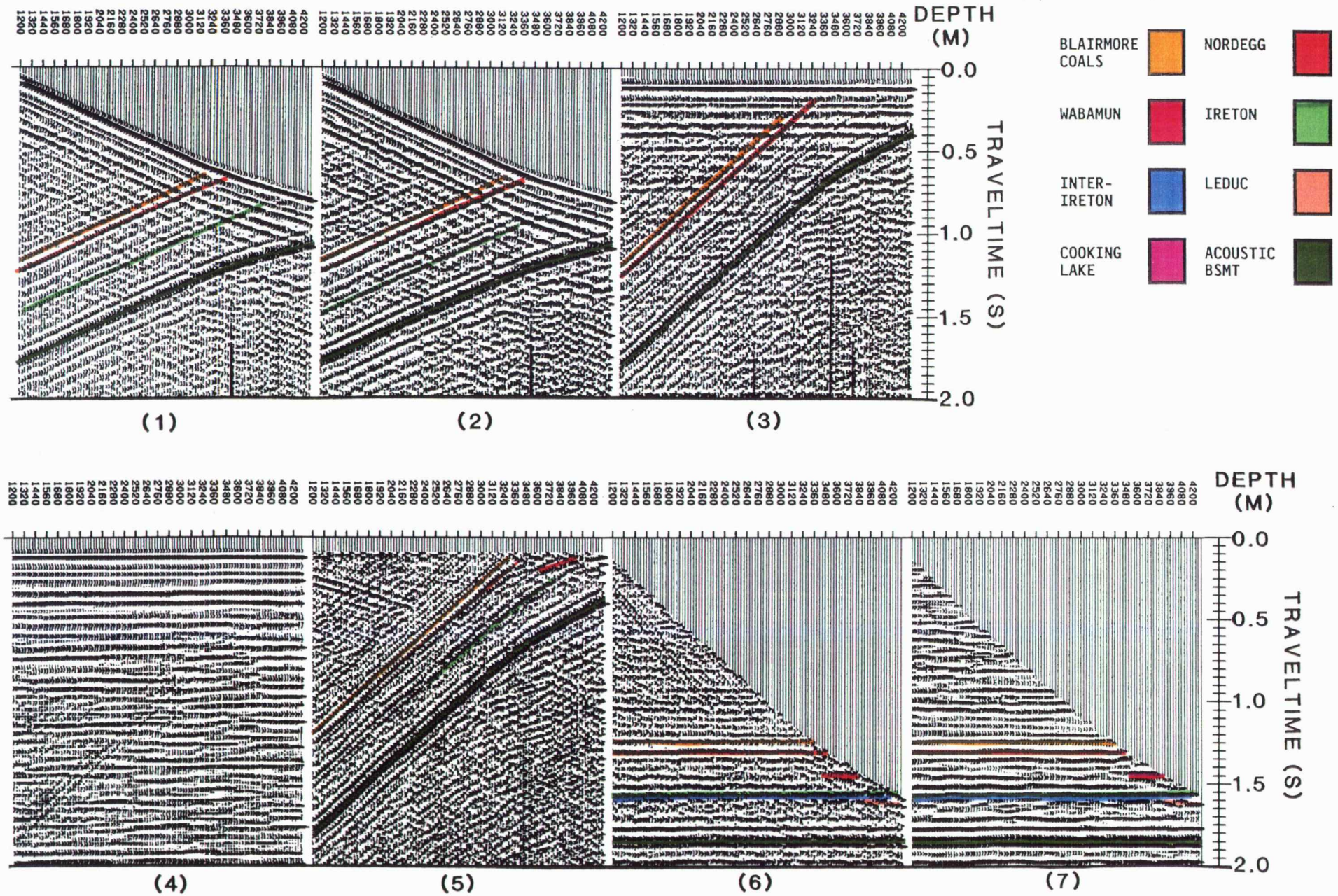
DEPTH
(M)
0.0
0.5
1.0
1.5
2.0
TRAVELTIME (S)
BLAIRMORE COALS
NORDEGG
WABAMUN
IRETON
INTER-IRETON
LEDUC
COOKING LAKE
ACOUSTIC BSMT
(1)
(2)
(3)
(4)
(5)
(6)
(7)

Figure 8.

DEPTH (M)
TRAVELTIME (S)
0.0
0.5
1.0
1.5
2.0
BLAIRMORE COALS
WABAMUN
INTER-IRETON
COOKING LAKE
NORDEGG
IRETON
LEDUC
ACOUSTIC BSMT
(1)
(2)
(3)
(4)
(5)
(6)
(7)

Figure 9.

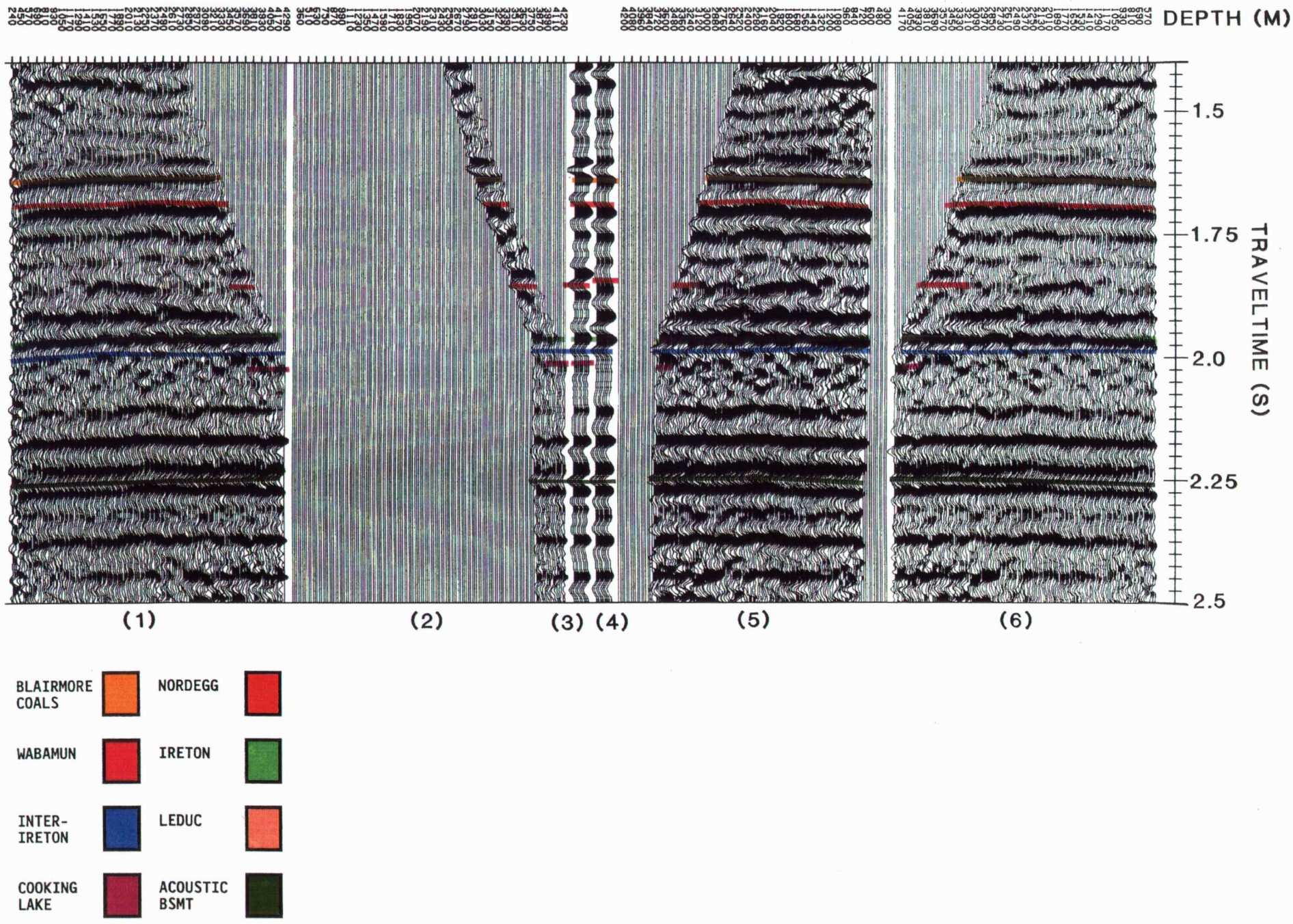
DEPTH (M)
1.5
1.75
2.0
2.25
2.5
TRAVELTIME (S)
(1)
(2)
(3)
(4)
(5)
(6)
BLAIRMORE COALS
NORDEGG
WABAMUN
IRETON
INTER-IRETON
LEDUC
COOKING LAKE
ACOUSTIC BSMT

Figure 10.

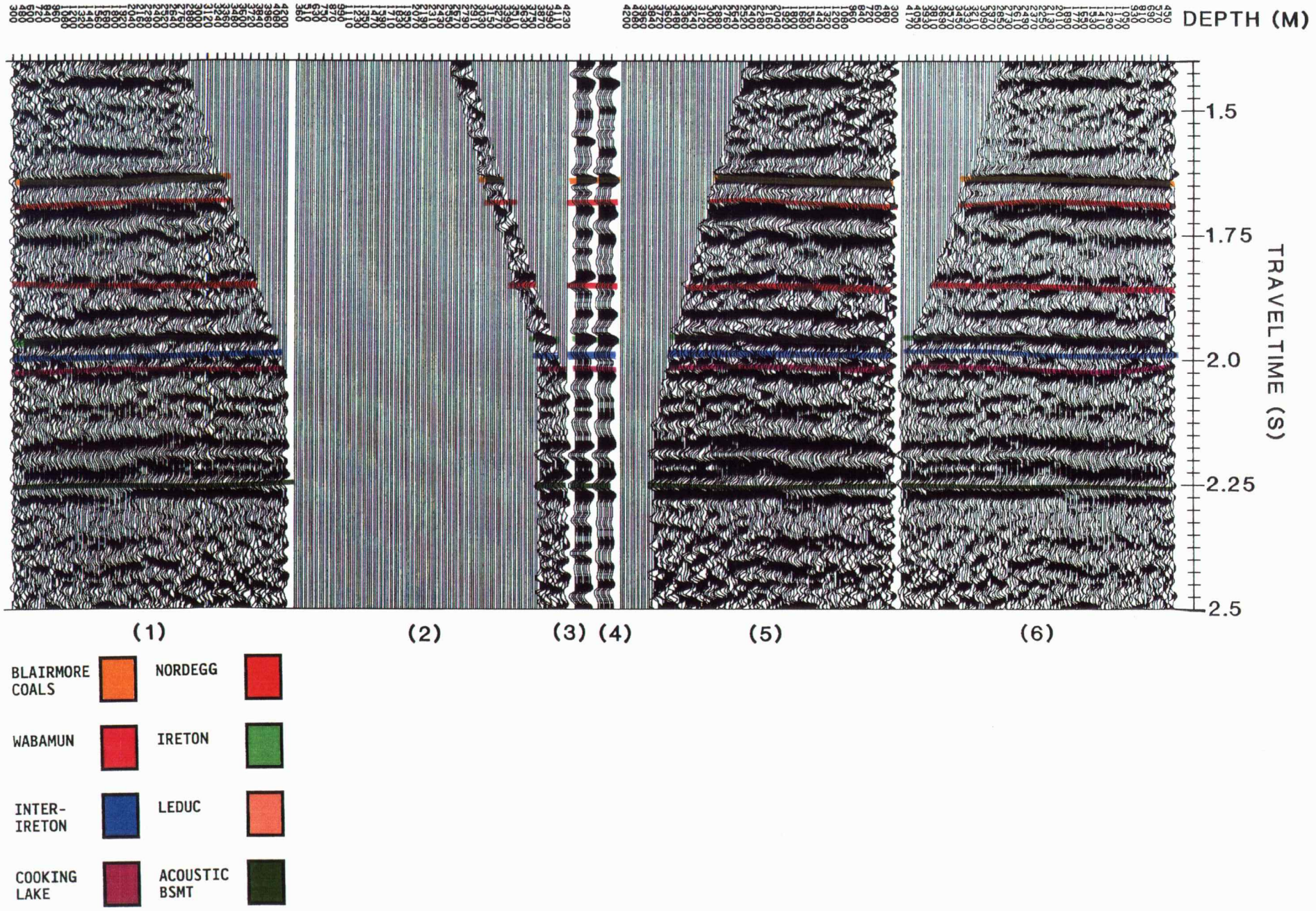
DEPTH (M)
TRAVELTIME (S)
1.5
1.75
2.0
2.25
2.5
(1)
(2)
(3)
(4)
(5)
(6)
BLAIRMORE COALS
NORDEGG
WABAMUN
IRETON
INTER-IRETON
LEDUC
COOKING LAKE
ACOUSTIC BSMT

Figure 11.

DEPTH (M)
FRT TRAVELTIME (S)
0.5
1.0
1.5
2.0
BLAIRMORE COALS
NORDEGG
WABAMUN
IRETON
INTER-IRETON
LEDUC
COOKING LAKE
ACOUSTIC BSMT
(1) X
(2) Y
(3) Z
(4) HMIN
(5) HMAX
(6) Z'
(7) HMAX'

Figure 12.

DEPTH (M)
TRAVELTIME (S)
0.5
1.0
1.5
2.0
BLAIRMORE COALS
NORDEGG
WABAMUN
IRETON
INTER-IRETON
LEDUC
COOKING LAKE
ACOUSTIC BSMT
(1)
(2)
(3)
(4)
(5)
(6)

Figure 13.

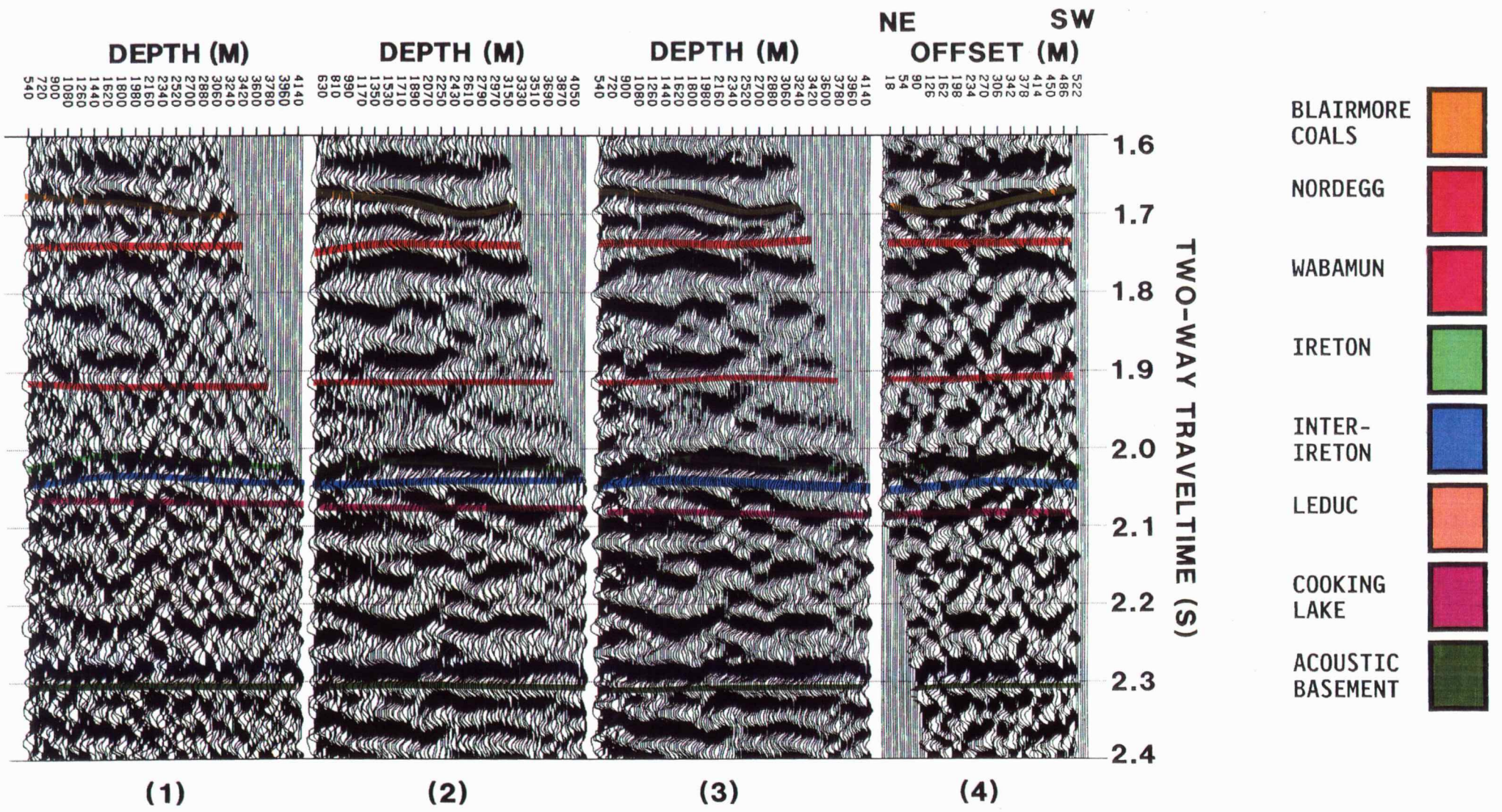
NE
SW
DEPTH (M)
DEPTH (M)
DEPTH (M)
OFFSET (M)
TWO-WAY TRAVELTIME (S)
1.6
1.7
1.8
1.9
2.0
2.1
2.2
2.3
2.4
(1)
(2)
(3)
(4)
BLAIRMORE COALS
NORDEGG
WABAMUN
IRETON
INTER-IRETON
LEDUC
COOKING LAKE
ACOUSTIC BASEMENT

Figure 14.

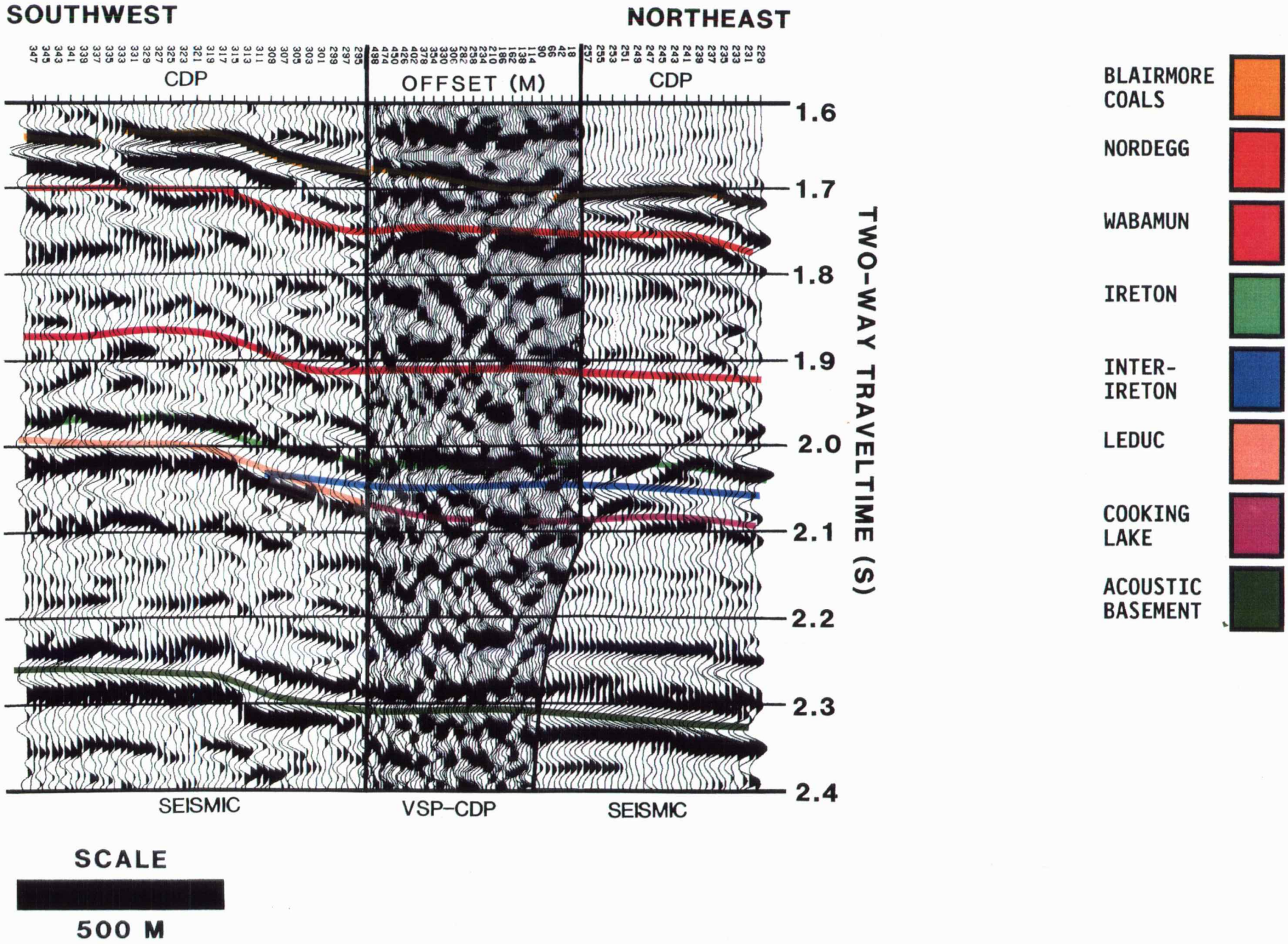
SOUTHWEST
NORTHEAST
CDP
OFFSET (M)
CDP
1.6
1.7
1.8
1.9
2.0
2.1
2.2
2.3
2.4
TWO-WAY TRAVELTIME (S)
SEISMIC
VSP-CDP
SEISMIC
SCALE
500 M
BLAIRMORE COALS
NORDEGG
WABAMUN
IRETON
INTER-IRETON
LEDUC
COOKING LAKE
ACOUSTIC BASEMENT

Figure 15.